Intermediate Temperature Strength Degradation in SiC/SiC Composites

G.N. Morscher[a] and J.D. Cawley[b]

[a] *Ohio Aerospace Institute (OAI), NASA Glenn Research Center, MS 106-5, Cleveland, OH 44135, USA*
[b] *Department of Materials Science and Engineering, Case Western Reserve University, Cleveland, OH 44106, USA*

ABSTRACT

Woven silicon carbide fiber-reinforced, silicon carbide matrix composites are leading candidate materials for an advanced jet engine combustor liner application. Although the use temperature in the hot region for this application is expected to exceed 1200°C, a potential life-limiting concern for this composite system exists at intermediate temperatures (800 +/- 200°C), where significant time-dependent strength degradation has been observed under stress-rupture loading. A number of factors control the degree of stress-rupture strength degradation, the major factor being the nature of the interphase separating the fiber and the matrix. BN interphases are superior to carbon interphases due to the slower oxidation kinetics of BN. A model for the intermediate temperature stress-rupture of SiC/BN/SiC composites is presented based on the observed mechanistic process that leads to strength degradation for the simple case of through-thickness matrix cracks. The approach taken has much in common with that used by Curtin and coworkers, for two different composite systems. The predictions of the model are in good agreement with the rupture data for stress-rupture of both precracked and as-produced composites. Also, three approaches that dramatically improve the intermediate temperature stress-rupture properties are described: Si-doped BN, fiber spreading, and "outside debonding".

1. Introduction and Review of Intermediate Temperature Stress-Rupture Behavior in Air

Non-oxide ceramic matrix composites (CMC's) such as SiC fiber-reinforced SiC matrix composites are envisioned for use as high-temperature, ≥ 1200°C, components of gas turbine engines [1-3]. However, there exists an intermediate temperature (600 to 1000°C)* regime where significant, time-dependent, strength degradation can occur [4]. Depending on the application, the intermediate temperature properties may be critical for success of that component. For example, the strength degradation at intermediate temperatures could be an issue for some applications, e.g. a cooled combustor liner [1], because the "cold side" of the combustor liner would be exposed to this temperature range, and this would be the portion of the combustor liner under the highest tensile stress. This is especially the case where the combustor liner would have to be attached to a metal frame. Therefore, it is important to understand and predict the time-dependent mechanical behavior at intermediate temperatures for design of these

* By intermediate temperature, we mean an elevated temperature below the supposed use temperature at which the material exhibits a minima in mechanical properties, i.e., what is sometimes called a "pest" condition [4].

composites in components, as well as for finding insights toward improvement of the intermediate temperature properties.

Oxidation of a non-oxide interphase that separates the fibers from the matrix is the primary reason that has been identified for intermediate temperature strength degradation. Carbon and BN have historically been the interphase materials of choice because they both enable the necessary mechanical properties, interfacial debonding and sliding, required to attain tough, composite behavior. However, both C and BN oxidize readily at temperatures greater than ~ 500°C. Carbon forms volatile CO and CO_2 species resulting in interphase recession at lower temperatures [5-6]. At higher temperatures, the gap left by the interphase can be filled with the SiO_2 oxidation product of the SiC fibers and matrix resulting in a strong oxide bond between the fiber and matrix [5]. BN oxidizes to form liquid B_2O_3 (boria). This results in the formation of a borosilicate glass at the interphase region when the boria reacts with the SiC fibers and matrix [7-8]. It also forms volatile hydrated species in the presence of water vapor [8].

The stress-rupture properties of composites with a carbon interphase have been shown to be inferior to composites with a BN interphase when tested in air [9-10]. The stress-rupture behavior of C and BN interphase single-tow minicomposites is shown in Figure 1 for precracked minicomposites reinforced with Nicalon™** (NIC in Figure 1a) and Hi-Nicalon™** (HN in Figure 1b) [10,11]. Note that the degradation in rupture properties due to the interphase is more severe for NIC reinforcement than for HN reinforcement. The air stress-rupture data available in the literature [4, 12-18] for C-interphase and BN-interphase data in the intermediate temperature regime are shown in Figure 2. Note that all of the C-interphase data are for NIC reinforcement and the BN interphase data set includes data from both HN and Sylramic®# (SYL in Figure 2) reinforced specimens. All of the C-NIC composites in Figure 2 had chemically vapor infiltrated (CVI) matrices whereas some of the BN interphase composites had silicon melt-infiltrated (MI) matrices.

Several mechanisms have been proposed for the observed strength degradation of C-interphase composites. First, dramatic interphase recession results in decoupled, long lengths of fibers. This weakens the composite because of the probabilistic nature of fiber failure, i.e. longer lengths of fibers fail at lower stresses [19]. Second, at higher temperatures, oxidation of the

** Nippon Carbon Co., Japan
# Dow Corning Corp., Midland, MI

fibers becomes significant and the oxide scale could act as a flaw. The time-dependence for stress-rupture was found to be in accord with this explanation for a (NIC), C interphase composite [12]. However, a third mechanism appears to often be important especially for composites consisting of the relatively unstable NIC fiber. This is the formation of new flaws on the surface of bare fiber after interphase recession [11]. This was suggested on the basis that the degradation in stress-rupture properties for NIC C-interphase composites were too severe compared to expectations for either of the first two mechanisms cited, and the fact that no discernable oxide scale growth could be measured for many of the conditions tested. Fiber surface modification that results in regions of C excess at the fiber surface of NIC fibers during chemical vapor infiltration (CVI) processing has been well documented [20]. This would not necessarily degrade the fiber strength at room temperature, but fiber strength degradation would occur if the oxidation of the local carbon formed a pit on the surface of the fiber. In addition, the intermediate temperature stress-rupture properties of composites with the more stable HN were not as poor and were more consistent with the above explanations (Figure 1).

BN interphases are superior to C interphases because the primary oxidation product of BN oxidation is a condensed phase, i.e., B_2O_3 liquid that eventually solidifies into a borosilicate glass as SiO_2 is added to the melt from oxidation of the SiC fibers and/or matrix, and B is leached from the melt from reaction with H_2O to form boron containing hydrated species [8]. The net result is very little if any decoupling of the fibers from the matrix so that the length of fiber carrying large stresses is confined to the region near the matrix crack. However, a significant reduction in the load carrying capability of the composite does occur, primarily due to strong bonding of the fibers to one another or to the matrix [17]. The inability of fibers to share loads globally when slight increases in applied stresses occur either due to external increases in stress or due to local increases in stress, e.g., near an individual fiber break (akin to Zhou and Curtin [21]), results in unbridged crack-growth and ultimately catastrophic failure.

This paper focuses on the factors and mechanisms that control intermediate temperature stress-rupture for BN interphase composites. A model that accounts for some of these factors will be presented. It will be shown to predict the intermediate temperature rupture data. Finally, recent enhancements to the microstructure of SiC/BN/SiC composites resulting in improved intermediate temperature composite performance will be presented. All of the stress-rupture data presented in this work that has not been published earlier was performed in the same manner as described in references 17 and 18. Woven composites, 150 mm in length, were tested in tension

where the ends of the specimens were "cold-gripped" and a slotted furnace with a 15 mm hot zone was inserted in the center region between the grips. The furnace was brought to temperature prior to the application of the load.

2. The Process of Intermediate Temperature Stress-Rupture of Woven BN Interphase Composites in Air

It was established in reference 17 from chemical analysis of fiber fracture surfaces (degree of fiber fracture surface oxidation) that whole areas of fibers in a matrix crack failed at the same time during the course of the stress-rupture experiment. It was also discerned from fracture mirror analysis of failed fibers that the amount of degradation to the fiber strength was commensurate with the expected amount from single fiber stress-rupture data [22]. That is no additional strength degradation occurred to the population of strongly bonded fibers. Therefore, failure under stress-rupture conditions at intermediate temperatures occurs by locally overloading due to the stress concentration associated with the strong bonding of fibers to the matrix. Not because the fibers are weakened. The depth of this embrittled region grows as the oxidation front moves deeper into the matrix crack (Figure 3). Eventually, one of the strongly bonded fibers breaks and causes all the other strongly bonded fibers to fail due to the inability to globally share the increased stress applied to the nearest neighbor fibers and unbridged crack growth. This view is strongly supported by the pattern of fracture mirrors from the strongly bonded regions of near fiber contact in the micrograph of Figure 3, which are indicative of correlated fiber failure. If the stress transferred to the pristine weakly bonded fibers cannot be carried by the remaining fibers, then the composite fails. Two criteria must be met in order for a composite to fail according to this process:

(1) A critical number of fibers in a given matrix crack must be strongly bonded to one another or to the matrix. When these fibers fail in a matrix crack, the stress increase to the remaining unbroken fibers is sufficient to cause them to fail.

(2) An event has to occur to fail one or more of those strongly bonded fibers to cause unbridged crack growth. Most likely, this event is caused by the failure of one strongly bonded fiber due to intrinsic fiber strength degradation (flaw growth) of a fiber that is relatively weak in the distribution of fiber strengths. It is also possible that fiber-

degradation could occur from fiber oxidation depending on the fiber-type and oxidizing environment.

The kinetics for fiber fusion or the depth into a matrix crack away from the exposed surface that fibers are strongly bonded depends on the ingress of oxidizing species into the matrix crack, i.e., the rate of oxide production, and the shortest distance between two fibers, i.e., the gap that must be filled by oxide. Ingress of oxidizing species can only occur if matrix cracks are present which intersect load-bearing fibers; therefore, fiber fusion will be dependent on the presence of matrix cracks, and whether or not those cracks are through the thickness of the specimen. The durability of the interphase will affect the rate for fiber-to-fiber fusion. It was found for the BN-HN-MI SiC matrix composites of reference 17 that the thin carbon layer that exists between the fiber and the BN due to fiber decomposition during matrix processing [23] enhances crack growth and interphase oxidation [18]. Also, the closer fibers are to one another or the thinner the interphase, the faster fibers will fuse to one another or to the matrix, respectively. Therefore, the uniformity of the interphase coating and the method of interphase coating will be critical. It was found in the earlier study [17] that over 95% of all the fibers were nearly in contact with one another, i.e. are separated by less than 100 nm, even though the average thickness of the interphase was 0.5 μm. This is especially a consequence of woven structures, where the act of weaving tightens tows and forces fibers into intimate contact with one another.

Fiber failure depends on the strength-distribution of the fibers in a matrix crack, the number of fibers in a matrix crack, and the effective gage length of loaded fibers. A wider distribution of fiber strengths for the same average strength will mean a greater probability for a fiber failure originating in the region exposed by a matrix crack. The number of fibers per tow, number of tows in a composite cross-section, and the size of the specimen for a given volume fraction of fibers will affect the total number of fibers in a matrix crack. The effective gage length of fibers will be controlled by the ability of the fibers to transfer load to the matrix, i.e., interfacial shear strength, the amount of interfacial recession that may occur, and the number of matrix cracks that are exposed in the "hot zone" of the furnace. An increase in the effective length of fully-loaded fibers will increase the likelihood that a strongly bonded fiber will fail in or near a matrix crack beginning the process of unbridged crack growth.

3. A Model For Intermediate Temperature Stress Rupture of SiC/BN/SiC Composites

In order to model this process, an approach conceptually similar to Curtin and coworkers [24-26] approach to model composite strength and individual fiber fracture was employed. Only the simple case of through-thickness cracks was considered. The model was applied to the two SiC fiber BN interphase MI SiC matrix systems plotted in Figure 2 by using available property information for these systems [16-18].

3.1 The Model

The stress on the fibers in a bridged matrix crack, σ_f, can be found from the applied far-field composite stress, σ, and the volume fraction of fibers in the loading direction, f.

$$\sigma_f = \frac{\sigma}{f} \tag{1}$$

With time, fibers exposed by a matrix crack will fail. Fiber failure is assumed to follow a Weibull distribution that can be used to determine the probability for fiber failure:

$$P(\sigma, L) = 1 - e^{-\phi} \tag{2}$$

ϕ is the fraction of failed fibers according to:

$$\phi = \frac{L}{L_o}\left(\frac{\sigma_f}{\sigma_o}\right)^m \tag{3}$$

where m is the Weibull modulus, σ_o is the reference stress and L_o is the reference length that corresponds to the average fiber strength determined in single fiber tensile tests. L is the effective gage length in the matrix crack. It proved useful to adopt the formulation of Curtin's [24] characteristic stress, σ_c, and characteristic gage length, δ_c, where $\phi(\sigma_c,\delta_c) = 1$ and δ_c is twice the

$$\sigma_c = \left(\frac{\sigma_o \tau L_o}{R}\right)^{\frac{1}{m+1}}; \qquad \delta_c = \frac{R\sigma_c}{\tau} \tag{4}$$

fiber slip length, by definition, R is the fiber diameter, and τ is the interfacial shear stress.

The fiber stress around the matrix crack varies because of load transfer due to friction (Figure 4). The fibers are subject to the maximum fiber stress in the crack opening. To determine the total fraction of fiber failures, ϕ can be integrated over the stress transfer length, $\Sigma\phi$, and added to the fraction of fiber failures in the crack opening width, ϕ_u:

$$\Sigma\phi = \int^{z} \phi dz = \int^{z} \left(\frac{\sigma(z)}{\sigma_o}\right)^m \frac{dz}{L_o} \tag{5a}$$

$$\phi_u = \left(\frac{u}{L_o}\right)\left(\frac{\sigma_f}{\sigma_o}\right)^m \tag{5b}$$

where z is the stress transfer length and u is the crack opening width which can be approximated by [27]:

$$u = \frac{\sigma^2 R}{4\tau f^2 E_f \left(1 + \frac{E_f f}{E_m(1-f)}\right)} \tag{6}$$

Equation 5a was solved by others [16, 17] for the case where z is equal to twice the fiber slip length, δ, assuming the far field stress on the fibers to be zero. This is an appropriate assumption because there is a negligible contribution to ϕ from the low far field fiber stress (~ 1/5 σ_{fc}). δ can then be approximated assuming a constant τ from the relationship (see Figure 4):

$$\delta = \frac{R\sigma_f}{\tau} \tag{7}$$

Equation 5a then simply becomes:

$$\phi(\delta) = \frac{\left(\frac{\sigma_f}{\sigma_c}\right)^{(m+1)}}{m+1} \tag{8}$$

The fraction of fibers that fail in a matrix crack can be determined by summing Equations 8 and 5b and simplifying with equation 4:

$$\phi_{t,T} = \frac{\left(\frac{\sigma_f}{\sigma_c}\right)^{(m+1)}}{m+1} + \frac{u}{L_o}\left(\frac{\sigma_f}{\sigma_o}\right)^m = \frac{1}{L_o}\left(\frac{\sigma_f}{\sigma_{o(t,T)}}\right)^m \left(\frac{\delta}{m+1} + u\right) = \frac{K_\phi}{\sigma^m_{o(t,T)}} \tag{9}$$

$$\text{where } K_\phi = \left(\frac{\sigma_f^m}{L_o}\right)\left(\frac{\delta}{m+1} + u\right) \tag{10}$$

The operative mechanism to be modeled to predict composite rupture is the failure of the strongly bonded fiber that triggers the growth of an unbridged crack through the embrittled fibers in a matrix crack. The time dependence for the depth of embrittlement into the composite determines the number of embrittled fibers available in a matrix crack. The time dependence for fiber-to-fiber fusion was determined empirically from examination of ruptured-specimen fracture surfaces for two of the MI composite systems [17,18] (Figure 5). It was found that a semi-empirical parabolic time-dependence was an adequate description:

$$x = C_{ox} t^{1/2} \tag{11}$$

where C_{ox} is an empirical coefficient that best fits the measured oxidation depth data for a given composite system.

Since the fiber strength degradation of pulled out fibers in a through-thickness cracked composite is consistent with the measured degradation in fiber strengths of as-produced fibers, the descriptive expression for time dependent fiber strength degradation developed by Yun and DiCarlo [22] for the latter was used. Their data for rupture strength of three SiC type fibers are plotted in Figure 5 as a Larson-Miller plot. The conditions for our study are indicated in Figure 6. This data was best fit, re-plotted on a stresss-time plot and re-fitted to fit the common form:

$$\sigma_{0(t,T)} = C_f \, t^{-1/n} \tag{12}$$

where C_f is the coefficient that best fits the fiber rupture data and n is the rupture exponent; both are dependent on the fiber type. This then becomes the time-dependent reference stress for equation 9.

One important factor for a fiber strength determination is the actual strength of the fibers in the composite after processing. The fiber strength of both the HN and SYL fibers at room temperature found by Yun and DiCarlo was 2800 MPa [22]. However, some strength degradation may occur due to composite processing. Curtin et al. [25] have established a composite ultimate-strength failure criterion based global load sharing assumptions:

$$\sigma_{ult} = \sigma_c \left[\frac{2(m+1)}{m(m+2)} \right]^{\frac{1}{m+1}} \left(\frac{m+1}{m+2} \right); \qquad \text{for } 2\delta > \rho_c^{-1} \tag{13}$$

Equation 13 is for matrix crack saturation where ρ_c is the crack density and ρ_c^{-1} would be the crack spacing. The room temperature ultimate strengths of all of the composites modeled in this study are known. Therefore, the ultimate strength of the fibers in the composites could be estimated by solving for σ_o from equations 13 and 4:

$$\sigma_{o(composite)} = \left[\frac{m(m+2)}{2(m+1)} \frac{R}{\tau L_o} \left(\frac{m+2}{m+1} \sigma_{ult} \right)^{m+1} \right]^{\frac{1}{m}} \tag{14}$$

Equation 11 is based on the room temperature ultimate fiber strength, $\sigma_{o(RT)}$, of 2800 MPa. Assuming the flaw growth mechanism that causes time-dependent fiber strength-degradation rate at intermediate temperatures is the same as for single fiber tests and depends on starting flaw size, the time-dependent fiber strength of fibers in the composite can be estimated from Equation 12:

$$\sigma_{0(t,T)} = \frac{\sigma_{o(composite)}}{\sigma_{o(RT)}} C_f \, t^{-1/n} = C_{frupture} t^{-1/n} \tag{15}$$

The fraction of fibers that fail in a matrix crack as a function of time can then be determined from equations 10 and 15 (Equation 16a). However, for the purpose of determining the fraction of fibers that fail as a function of the depth of oxidation embrittlement, it is advantageous to convert t into depth, x, from equation 11 as well (Equation 16b).

$$\phi_{t,T} = \frac{K_\phi}{C^m_{frupture}} (t)^{m/n} \tag{16a}$$

$$\phi_{t,T} = \frac{K_\phi}{C^m_{frupture}} \left(\frac{x}{C_{ox}} \right)^{2m/n} \tag{16b}$$

At this point it is illustrative to show the probability for fiber failure from Equations 16a and 16b and the number of predicted fiber failures in and around a single matrix crack for various applied rupture stress conditions for the HN-BN-MI [17] composite system as a function of time and depth of embrittlement (Figure 7a and b, respectively). The variables used are listed in Table I. Most fiber failure would occur at short times and diminish with increasing time (Figure 7a); however, it takes a period of time to embrittle most fibers. For this reason, when predicting whether or not a fiber failure will occur for an embrittled fiber, it is absolutely necessary to take into account the probability that fibers had already failed prior to being embrittled. Figure 7 depicts the situation where rupture time reaches 21.5 hours (the time to fully embrittle the HN-BN-MI composite at 815°C in air). At a depth of 0.2 mm from the composite surface, fibers were not embrittled for 0.9 hours. However, a greater fraction of fibers would be expected to fail prior to fiber embrittlement at 0.2 mm depth, ϕ_t, compared to the

fraction of fibers that would be expected to fail after embrittlement, ϕ_{emb}. If fibers fail prior to embrittlement then the load shed from that fiber is shared globally, unbridged crack growth will not occur, and those fibers that fail prior to embrittlement are removed from the population of weak fibers that could fail. Therefore, the fraction of embrittled fibers that fail at a given region in a matrix crack can be estimated according to the construct of Figure 7 using Equation 16b for embrittlement depth:

$$\phi_{emb} = \phi_{t\max} - \phi_t = \frac{K_\phi}{C_{frupture}^m C_{ox}^{2m/n}}\left[x_{\max}^{2m/n} - x^{2m/n}\right] \tag{17}$$

where ϕ_{tmax} is the fraction of fibers that fail at the maximum time and ϕ_t is the fraction of fibers that failed prior to the time of embrittlement. The number of embrittled fiber failures can then be determined from the product of the number of fibers per unit thickness, $\overline{N}_x$, and the integration of ϕ_{emb} over the maximum depth of oxidation embrittlement, x_{max}:

$$N_{femb}^{t<t_{emb}} = \overline{N}_x \int_0^{x_{\max}} \phi_{emb} dx = \frac{\overline{N} x C_\phi}{C_{frupture}^m C_{ox}^{2m/n}} x_{\max}^{\left(\frac{2m}{n}+1\right)}\left[1 - \frac{1}{\frac{2m}{n}+1}\right] \tag{18}$$

This equation is valid up to the time that all of the fibers throughout the entire matrix cross-section have been embrittled, t_{emb}. If no embrittled fibers failed prior to the time it takes to strongly bond all of the fibers in a through-thickness crack, the number of embrittled fiber failures would be equal to:

$$N_{femb}^{t>t_{emb}} = N_{femb}^{t<t_{emb}} + N_f\left(\phi_t - \phi_{t_{emb}}\right) = N_{femb}^{t<t_{emb}} + N_f \frac{K\phi}{C_{frupture}^m}\left(t^{m/n} - t_{emb}^{m/n}\right); \text{ for } t > t_{emb} \tag{19}$$

where N_f is the total number of fibers in the composite cross-section.

When a strongly bonded fiber fails at time t_{ffail}, it will be assumed that all of the embrittled fibers fail in the cross-section of the matrix crack. Then, if the load shed onto the remaining pristine fibers cannot be carried by the remaining fibers, the composite will rupture. The ultimate stress-criterion (Curtin et al [25]) for most conditions will be for the case of a composite that is not crack-saturated:

$$\sigma_{ult} = \sigma_c e^{\frac{1}{m+1}}; \qquad \text{for } 2\delta < \rho_c^{-1} \tag{20}$$

where $\sigma_{o(t,T)}$ must be used as the reference stress in the determination of σ_c (Equation 4). If the matrix were saturated with matrix cracks Equation 13 would be used. The stress remaining on pristine fibers can be determined from:

$$\sigma_{ffail} = \frac{\sigma_f}{1 - f_{emb}} \tag{21}$$

where

$$f_{emb} = \frac{2x_{t_{ffail}}}{b} \tag{22}$$

If $\sigma_{ffail} > \sigma_{ult}$, then the composite fails.

One further consideration must be taken into account. All of the analysis up to this point has been for the case of a single matrix crack. Most of the specimens tested in rupture have several matrix cracks exposed to the hot zone depending on the crack-density associated with the applied stress condition. An increase in crack density increases the effective gage length of strongly bonded fibers, and thereby the fraction of fiber failures. To account for this, all that is required is to multiply f_{emb} by the number of cracks, N_c, which results in:

$$N_{femb} = N_c N_{femb(\text{single crack})} \tag{23}$$

where $N_{femb(\text{single crack})}$ is the solution to either equation 18 or 19, depending on the time, and Nc can be found from:

$$N_c = \rho_c L_g \tag{24}$$

where L_g is the gage length, i.e. the length of specimen in the hot zone.

3.2 Applying the Model

It was decided to model two regimes of rupture behavior rather than the entire rupture curve: (a) "oxidation kinetics" controlled rupture and (b) "single fiber failure" controlled rupture. The first case is where many fibers break during the rupture condition due to higher applied stresses and high crack densities. The latter condition is the case where the first embrittled fiber to break in a composite causes ultimate composite failure. The entire rupture curve could be modeled similar to Lara-Curzio [12] in an iterative fashion where a computer program essentially continues to increase time in discrete steps and solves the above equations in order to

determine if the equation $\sigma_{ffail} > \sigma_{ult}$ is fulfilled for a given stress/crack-density condition [29]. However, for the case of several matrix cracks in a hot zone, after first fiber failure, each crack has to be treated independently and there exists an intermediate stress range where higher applied stresses will yield longer rupture times than lower applied stress conditions*. This may actually be indicative of some of the scatter in rupture results; however, what is usually considered to be of greatest importance is the "run-out" stress condition, i.e. case (b) above, which the single fiber failure condition would predict. Therefore, rupture curves will be predicted for these two extremes and the switch from the kinetic-dependence to single fiber failure controlled rupture occurs at the point where single fiber failure rupture predicts longer times for rupture.

Case (a) can simply be determined by finding the time that satisfies the condition where equation 20 and equation 21 are equal and is controlled by the time-dependent embrittlement depth. Case (b) was determined by solving for the case where equation 23 is equal to 1, i.e., the first embrittled fiber failure in a matrix crack. Case (b) requires an accurate measure of crack-density as a function of the stress-state. This information was available for the HN-BN-MI SiC and SYL-BN-MI SiC systems [17,18]. Figure 8 shows the predictions for the two composite systems and the actual rupture data from references 16 through 18. Table I lists the experimentally determined variables that went into the model for both systems and Figure 9 shows the stress-dependent crack density as determined from measured crack densities from some of the rupture specimens.

The two extremes predict the rupture behavior relatively well. The kinetic-limit seems to overestimate rupture time slightly. One possible reason for this overestimate is the presence of a possible stress-concentration on the outer perimeter of bridging fibers in a matrix crack [30,31], which was not taken into account in the model#. The model also slightly underestimates the rupture times for the SYL composites for the single fiber limit. One issue with SYL fiber composites in general is a relatively high τ and the possibility that minor to moderate local load sharing conditions exist even for room temperature failure. If this is the case, the ultimate

* For example, for a higher stress condition, first embrittled fiber failure occurs at a time less than at a lower stress condition. However, the shorter-time-first-embrittled-fiber-failure may not be at a condition where ultimate composite failure would occur, i.e. x is too small to satisfy $\sigma_{ffail} > \sigma_{ult}$, and one would have to "wait" until another fiber fails in that specific matrix crack for ultimate failure to occur. It is possible that the time for the lower stress condition first embrittled fiber failure to be less than the second fiber failure of the higher stress condition and sufficient for ultimate composite failure [29]. (It should be noted that the determination of ϕ_{emb} in reference 29 is inappropriate under this scenario, the analysis used here should be used instead.)

For the model developed by Evans et al [31] of a C interphase composite system, fiber degradation was due to oxide scale growth and unbridged crack growth was due to fiber failure at the perimeter of the matrix crack due to the increased stress-concentration of the unbridged crack. A fundamental difference with the model proposed here is that an interior strongly bonded fiber can trigger the failure of the entire region of strongly bonded fibers.

strength of the fibers in the as-produced composite, $\sigma_{o(composite)}$, would be underestimated from the composite ultimate strength, σ_{ult} (Equation 14), which was based on global load sharing assumptions. This would effectively reduce the estimated time-dependent fiber strength and predict shorter rupture times for a given stress.

The model predicts a fiber gage-length dependence for stress-rupture. This provides an opportunity to independently test model predictions. This was verified by precracking composites at room temperature so that they possess a larger crack density than that from stress-rupture at an applied stress less than the precrack condition. For the HN-BN-MI specimen, some precracked experiments were performed. A precrack stress of 200 MPa was performed at room temperature and then the specimen was subjected to stress-rupture at a lower stress. This precrack condition resulted in a crack density of ~ 2 cracks/mm. The increased lengths of loaded fibers resulted in significantly shorter rupture times at lower stresses than the specimens that were not precracked as the model also predicted fairly well. The run-out stress was slightly underestimated by the model. However, the model effectively predicted the decrease in stress-rupture time with increasing crack density.

4.0 Improvements in Intermediate Temperature Stress-Rupture of SiC/BN/SiC Composites

Based on the understanding of the mechanistic process leading to intermediate temperature stress-rupture, in part derived from the development and verification of the above model, a few approaches have been employed to improve intermediate temperature stress-rupture. The most desirable would to use a more durable interphase than BN. However, to date, no real interphase has presented itself, but the BN can be improved. For example, composites with higher BN processing temperature or BN doped with Si have shown greater resistance to oxygen and water containing environments at intermediate temperatures [32]. Si-doped BN was especially resistant to these environments; however, it requires processing temperatures on the order of 1400°C, too high for processing of preforms. Some progress has been made with coating large individual pieces of woven cloth with the higher processing temperature Si-doped BN interphase and then stacking the woven cloth to fabricate MI composites [33].

Since fiber separation is one of the controlling factors in fiber-to-fiber fusion, one logical technique to slow this process down would be to spread fibers further apart. By increasing the time for fiber fusion, more fibers would fail in a matrix crack under global load sharing conditions, thereby reducing the available fibers that could fail after fibers are strongly bonded to

one another or to the matrix. Two techniques have enabled fiber spreading that results in greater fiber-to-fiber separation: mechanical "fluffing" of woven fabric [34] and heat-treating woven fabric to produce a ~ 100 nm thick in-situ BN layer on the fibers [35]. The former mechanically separates fibers, the latter produces a high-temperature BN layer that separates fibers by an additional 200 nm. The in-situ BN Sylramic® fibers are referred to as SYL-iBN.

Another improvement has been to alter the interface where interface debonding and sliding occur within the interphase region from the fiber/BN interface to the BN/matrix interface, i.e., "outside debonding" [36]. This would be similar in concept to multi-layer coatings [37] where interphase oxidation is engineered to occur as far away from the fiber surface as possible. The multi-layer C/SiC interphase coating of NIC/SiC composites in reference 37 does show slight improvement over other C-interphase NIC/SiC composites at intermediate temperatures in air (Figure 2). For "outside debonding" BN interphases, oxygen and water vapor do not have direct access to the fibers. In order to fuse fibers to the matrix or to one another, oxidation must occur through the thickness of the BN, which is relatively slow because the boria reacts with the SiC in the matrix crack to effectively seal the matrix crack.

All three of the above approaches have been demonstrated for SYL reinforced composites. Figure 10 shows the dramatic improvements in intermediate stress rupture properties for the three approaches described above in comparison to the data from the material modeled in Figure 7 [16-18]. 500-hour rupture stresses in excess of 200 MPa were common for all three of the approaches, the "outside debonding" and Si-doped BN interphase composites performed the best. Precrack experiments were performed for fiber-spread composites and for "outside debonding" composites in reference 36 (Figure 11). The fiber-spread composites did show a decrease in stress-rupture properties with increased crack density whereas the "outside debonding" composites did not, in fact "outside debonding" composites showed improvement. In other words, stress-rupture of fiber-spread composites still possess a "gage-length" dependence whereas for "outside debonding" this does not appear to be the case. The kinetic limit as determined for the composites modeled in Figure 7b no longer applies to either of these cases (Figure 11) and a new time-dependence for fiber embrittlement would have to be determined in order to model these composites. It obviously takes a longer time to fuse fibers together that have longer separation distances. "Outside debonding" composites appear to be controlled by the time it takes to oxidize through the BN interphase layer, approximately 100 hours at 815°C in air.

CONCLUSIONS

Intermediate temperature strength degradation of SiC/SiC composites is due to a "pest" condition primarily caused by the oxidation of the interphase separating the fibers and the matrix. Although, BN interphases are superior to carbon interphase composites, they still exhibit significant degradation in stress-rupture properties at intermediate temperatures. The main factor causing this strength degradation is the fusion of fibers to one another in a matrix crack that is exposed to the oxidizing environment. The amount of strength degradation is dependent on the kinetics for fusion of fibers to one another, the number of matrix cracks, and the applied stress state. It was shown that the stress-rupture properties of SiC/BN/SiC composites could be effectively modeled using an approach that considers the probability of fiber failure in relation to the likelihood that the fiber had already been fused to its neighbor or the matrix. One important aspect of the model that was verified was the increased susceptibility to stress-rupture for composites with a greater number of matrix cracks.

Recently, improvements have been made for BN-interphase composites. These include, Si-doped BN, composites with more effective fiber spreading, and BN interphases where the debonding and sliding occur between the BN layer and the matrix rather than the fiber and the BN layer. Consistent with the mechanistics assumed in the model, for composites made with these modifications, the 500-hour rupture stress increased from about 155 MPa for conventional composites to over 200 MPa. For "outside debonding", 500-hour rupture stresses close to 250 MPa have been attained. This does not necessarily eliminate the "pest regime" for these composites; however, these approaches would significantly increase the stress range these composites could withstand at intermediate temperatures in oxidizing environments.

REFERENCES:

1. Brewer, D., HSR/EPM Combustor Materials Development Program . *Mater. Sci. Eng. A*, 1999, **A261**, 284-291.
2. Grondahl, C.M., and Tsuchiya, T., Performance benefit assessment of ceramic components in a MS9001FA gas turbine, 1998, ASME. 98-GT-186.
3. Kameda, T., Itoh, Y., Hishata, T, and Okamura, T., Development of continuous fiber reinforced reaction sintered silicon carbide matrix composite for gas turbine hot parts application. 2000, ASME, 2000-GT-67.
4. Heredia, F.E., McNulty, J.C., Zok, F.W., and Evans, A.G., Oxidation embrittlement probe for ceramic-matrix composites. *J. Am. Ceram. Soc.*, 1995, **78**, 2097.
5. Filipuzzi, L., Camus, G., Naslain, R., and Thebault, J., Oxidation mechanisms and kinetics of 1D-SiC/C/SiC composite materials: I, an experimental approach. *J. Am. Ceram. Soc.*, 1994, 77, 459-466.

6. Eckel, A.J., Cawley, J.D., and Parthasarathy, T., Oxidation of a continuous carbon phase in a nonreactive matrix. *J. Am. Ceram. Soc.*, 1995, **78**, 972-980.
7. Sheldon, B.W., Sun, E.Y., Nutt, S.R., and Brennan, J.J., Oxidation of BN-coated SiC fibers in ceramic-matrix composites, *J. Am. Ceram. Soc.*, 1996, **79**, 539-43.
8. Jacobson, N.S., Morscher, G.N., Bryant, D.R., and Tressler, R.E., "High-temperature oxidation of boron nitride: II, boron nitride layers in composites. *J. Am. Ceram. Soc.*, 1999, **82**, 1473-82.
9. Lin, H.T. and Becher, P.F., Effect of coating on lifetime of Nicalon fiber-silicon carbide composites in air. *Materials Science and Engineering*, 1997, **A231**, 143-150
10. Morscher, G.N., Tensile stress-rupture of SiC_f/SiC_m minicomposites with carbon and boron nitride interphases at elevated temperatures in air. *J. Am. Ceram. Soc.*, 1997, **80**, 2029-42.
11. Martinez-Fernandez, J. and Morscher, G.N., Room and elevated temperature tensile properties of single tow Hi-Nicalon, carbon interphase CVI SiC matrix minicomposites. *J. European Ceram. Soc.*, **20**, 2627-2636.
12. Lara-Curzio, E., Stress-rupture of Nicalon/SiC continuous fiber ceramic matrix composites in air at 950oC. *J. Am. Ceram. Soc.*, 1997, **80**, 3268-3272
13. Lipetzky, P., Stoloff, N.S., and Dvorak, G.J., Atmospheric effects on high-temperature lifetime of ceramic composites. *Ceram. Eng. Sci. Proc.*, 1997, **18**, 355-362.
14. Verrilli, M.J., Calomino, A.M., and Brewer, D.N., Creep-rupture behavior of a Nicalon/SiC composite. In *Thermal and Mechanical Test Methods and Behavior of Continuous-Fiber Ceramic Composites* (ASTM STP 1309), ed. M.G. Jenkins, S.T. Gonczy, E. Lara-Curzio, N.E. Ashbaugh, and L. Zawada. ASTM, 1997, pp. 158-175.
15. Steyer, T.E., Zok, F.W., and Walls, D.P., Stress rupture of an enhanced Nicalon™/SiC composite at intermediate temperatures. *J. Am. Ceram. Soc.*, 1998, **81**, 2140-2146.
16. Brewer, D., Calomino, A.M., and Verilli, M.J., unpublished research.
17. Morscher, G.N., Hurst, J., and Brewer, D., Intermediate-temperature stress rupture of a woven Hi-Nicalon, BN-interphase, SiC-matrix composite in air. *J. Am. Ceram. Soc.*, 2000, **83**, 1441-49.
18. Morscher, G.N. and Hurst, J., Stress-rupture and stress-relaxation of SiC/SiC composites at intermediate temperature, Ceram. Eng. Sci. Proc., 2001, **22**, in print.
19. Lara-Curzio, E., Ferber, M.K., and Tortorelli, P.F., Interface oxidation and stress-rupture of Nicalon/SiC CFCC's at intermediate temperatures. Key Engineering Materials, Vols. 127-131. Trans. Tech. Publications, Switzerland, 1997, pp. 1069-1082.
20. Naslain, R., Fiber-matrix interphases and interfaces in ceramic matrix composites processed by CVI. *Composite Interfaces*, 1993, **1**, 253-286.
21. Zhou, S.J. and Curtin, W.A., Failure of fiber composites: a lattice Green function model. *Acta Metall. Mater*, 1995, **42**, 3093-104.
22. Yun, H.M. and DiCarlo, J.A., Time/temperature dependent tensile strength of SiC and Al2O3-based fibers, in Ceramic Transactions, Vol. 74, Advances in Ceramic-Matrix Composites III. Eds. N. P. Bansal and J.P. Singh. American Ceramic Society, Westerville OH, 1996, pp. 17-26.
23. Ogbuji, L. U. J. T. , Identification of a Carbon Sublayer in a Hi-Nicalon/BN/SiC Composite, *J. Mater. Sci. Letters*. 1999, **18**, 1825-1827.
24. Curtin, W.A., Multiple matrix crack spacing in brittle matrix composites. *J. Am. Ceram. Soc.*, 1991, **74**, 2837.
25. Curtin, W.A., Ahn, B.K., and Takeda, N., Modeling brittle and tough stress-strain behavior in unidirectional ceramic matrix composites, *Acta mater.*, 1998, **46**, 3409-3420.
26. Iyengar, N. and Curtin, W.A., Time-dependent failure in fiber-reinforced composites by fiber degradation. *Acta mater.*, 1997, **45**, 1489.
27. Marshall, D.B., Cox, B.N., and Evans, A.G., The mechanics of matrix cracking in brittle-matrix fiber composites. *Acta metal.*, 1985, **33**, 2013-2021.
28. Cao, H. and Thouless, M.D., Tensile tests of ceramic-matrix composites: theory and experiment. *J. Am. Ceram. Soc.*, 1990, **73**, 2091-2094.
29. Morscher, G.N., Intermediate temperature stress rupture of SiC fiber, SiC matrix composites in air. Ph. D. Thesis, Case Western Reserve University, Cleveland, Ohio. 2000.

30. Xia, Z.C., Hutchinson, J.W., Evans, A.G., and Budiansky, B., On large scale sliding in fiber-reinforced composites. *J. Mech. Phys.Solids*, 1994, **42**, 1139-58.
31. Evans, A.G., Zok, F.W., McMeeking, R.M., and Du, Z.Z., Models of high-temperature, environmentally assisted embrittlement in ceramic-matrix composites. *J. Am. Ceram. Soc.*, 1996, **79**, 2345-2352.
32. Morscher, G.N., Bryant, D., and Tressler, R.E., Environmental durability of BN-based interphases (for SiCf/SiCm composites) in H_2O containing atmospheres at intermediate temperatures. *Ceram. Eng. Sci. Proc.*, 1997, **18**, 525-533.
33. Morscher, G.N., Yun, H.M., and Hurwitz, F., High-temperature Si-doped BN interphases for woven SiC/SiC composites, *Ceram. Eng. Sci. Proc.*, 2002, submitted.
34. Calomino, A. and Brewer, D., unpublished research.
35. Yun, H.M. and DiCarlo, J.A., Thermostructural behavior of SiC fiber fabrics and implications for CMC. *Ceram. Eng. Sci. Proc.*, 2000, **21**, 347-362.
36. Morscher, G.N., Yun, H.M., DiCarlo, J.A., and Thomas-Ogbuji, L., Outside debonding of the BN interphase in SiC/SiC composites. *Ceram. Eng. Sci. Proc.*, 2002, submitted.
37. Pasquier, S., Lamon, J., and Naslain, R., Static fatigue of 2D SiC/SiC composites with multilayered (PyC-SiC)n interphases at high temperatures in air. in Key Engineering Materials, Vols. 164-165, 1999, Trans. Tech Publications, Switzerland., pp. 249-252.

Table I: Composite and constituent properties.

	HN	SYL
Composite Physical Properties		
Tow ends per cm	6.7	7.1
No. Plies	8	8
Thickness, mm	2.1	2.1
Width, mm	12.5	10
No. fibers per tow	500	800
R, μm	6.5	5
F	0.17	0.17
Composite Mechanical Properties		
E_c, GPa	215	265
ν	0.15	0.15
Room Temperature σ_{ult}	390	340
τ, MPa	30	60
E_f, GPa	280	380
E_m, GPa	202	242
Fiber Strength Distribution Properties		
σ_o, MPa	2,800	2,800
M	7	5
L_o, mm	25.4	25.4
Time Dependent Properties		
C_{ox}	0.215	0.125
C_f	1761	2169
n	56.5	122

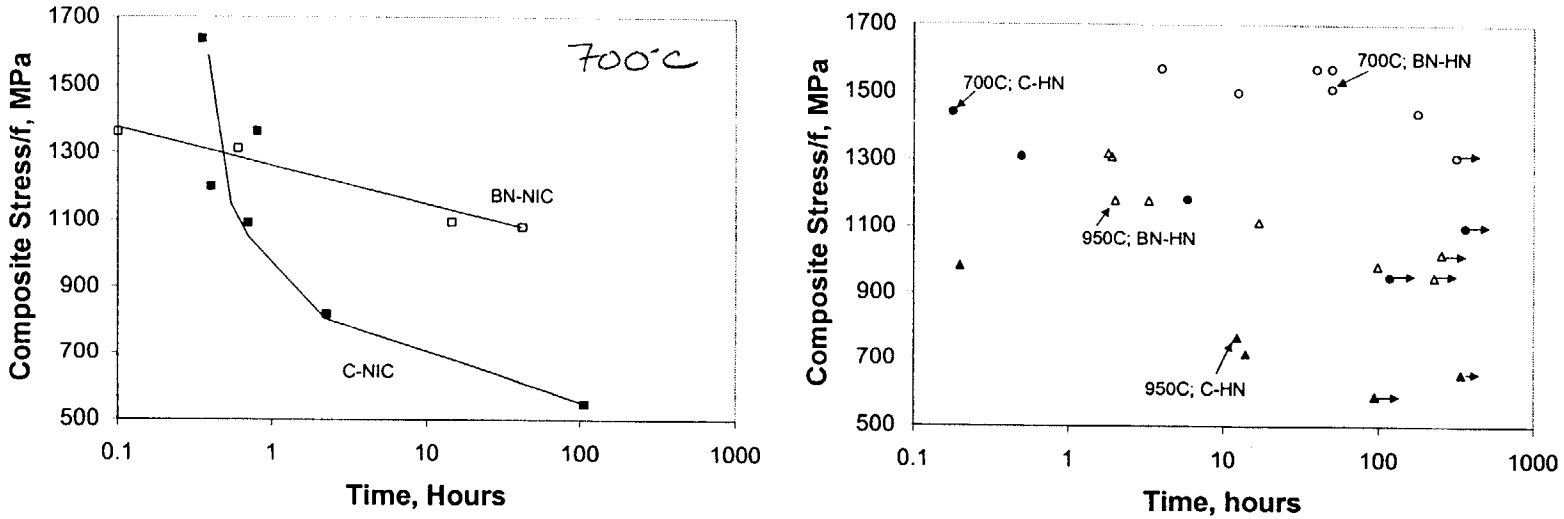

Figure 1: Stress-rupture in air of precracked minicomposites with C or BN interphases for (a) NIC fiber minicomposites and HN minicomposites. (data reproduced from references 10 and 11).

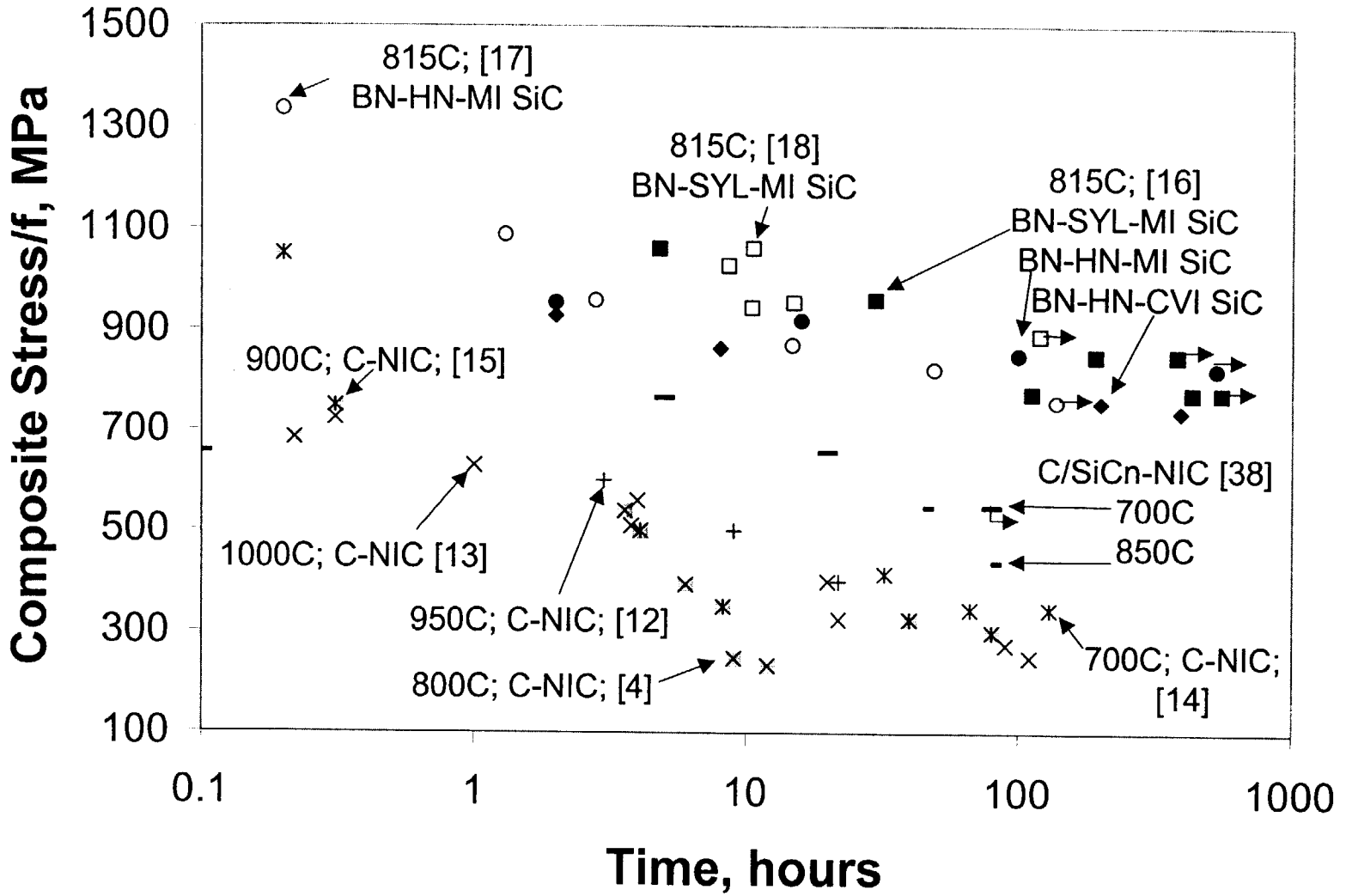

Figure 2: Stress-rupture data in air for woven SiC/SiC composites. The applied stress was normalized by the volume fraction of fibers in the loading direction in order to compare all the data.

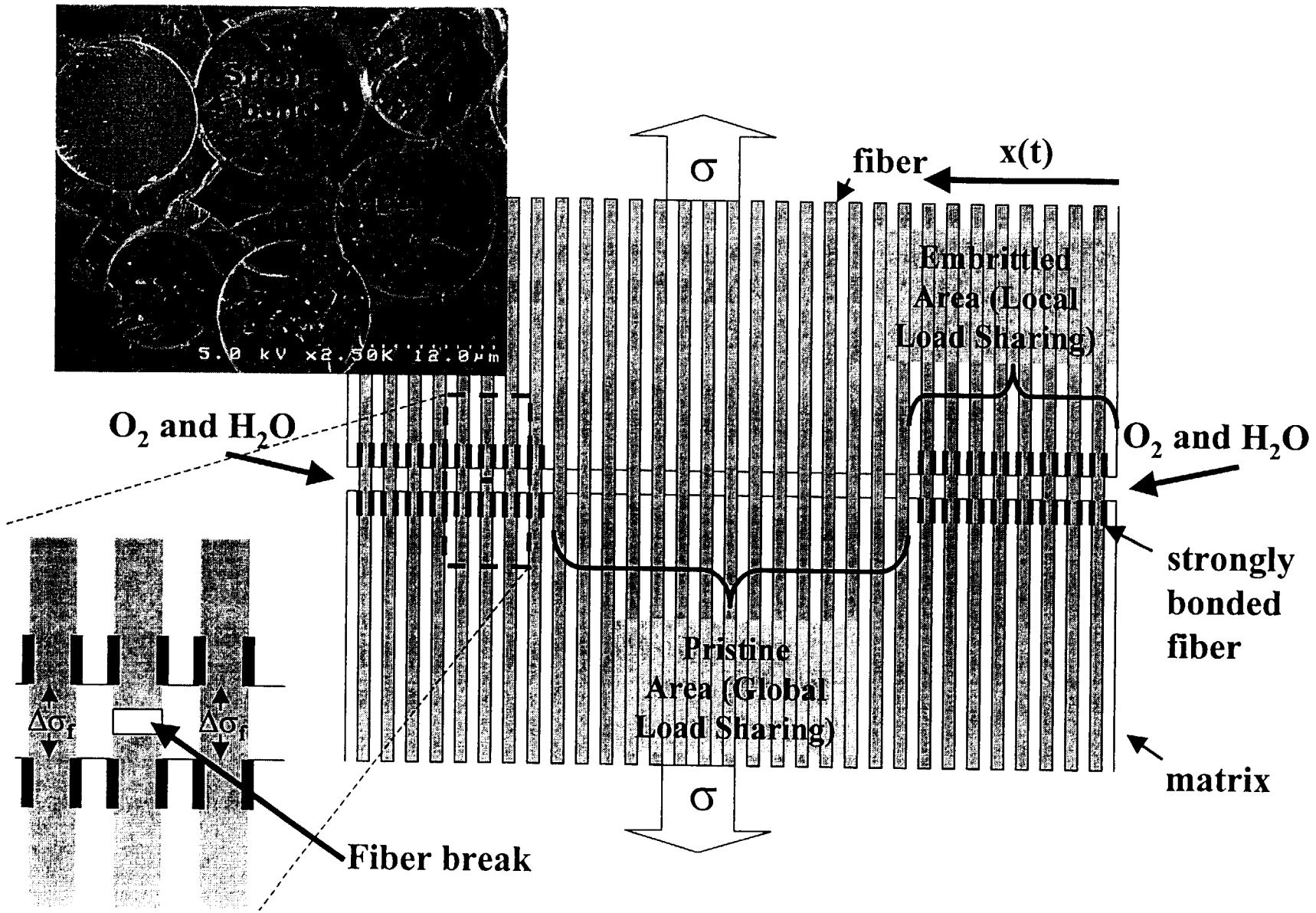

Figure 3: Idealized schematic representation of oxygen ingress in a matrix crack and an individual fiber failure that leads to failure of all strongly bonded fibers. An example of which is given in the upper left hand corner for a HN/BN/MI SiC composite.

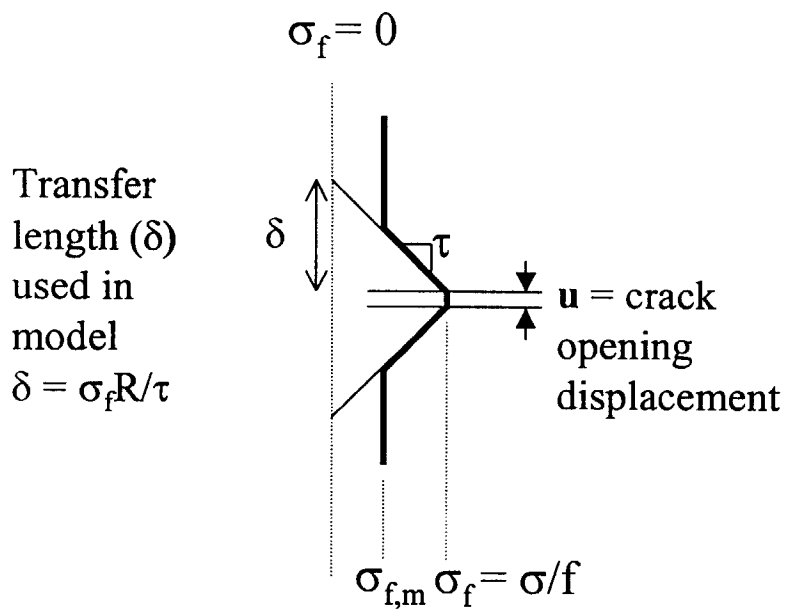

Figure 4: Schematic representation of stress-profile at and around a matrix crack in a composite. $\sigma_{f,m}$ would represent the stress on the fibers where the fibers and the matrix share the load according to the rule of mixtures. The model assumes δ extends to $\sigma_f = 0$ for simplicity (Equation 7).

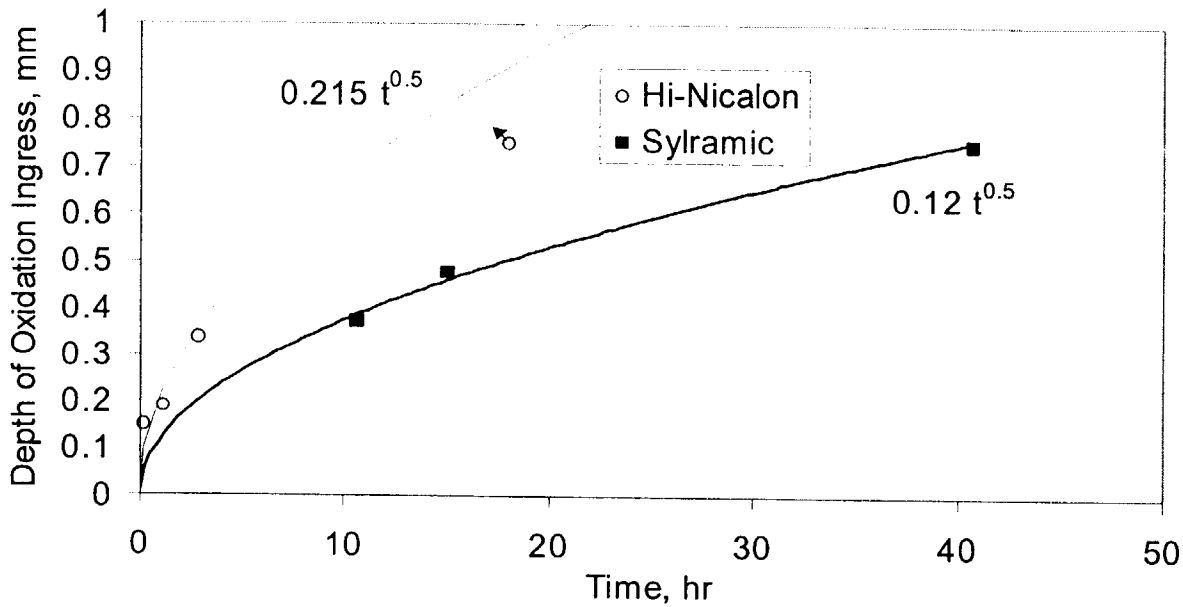

Figure 5: Depth of oxidation into the specimen from the surface of the composite versus rupture time for 815°C rupture of BN interphase, MI SiC composites. The specimen widths were approximately 2 mm [17,18].

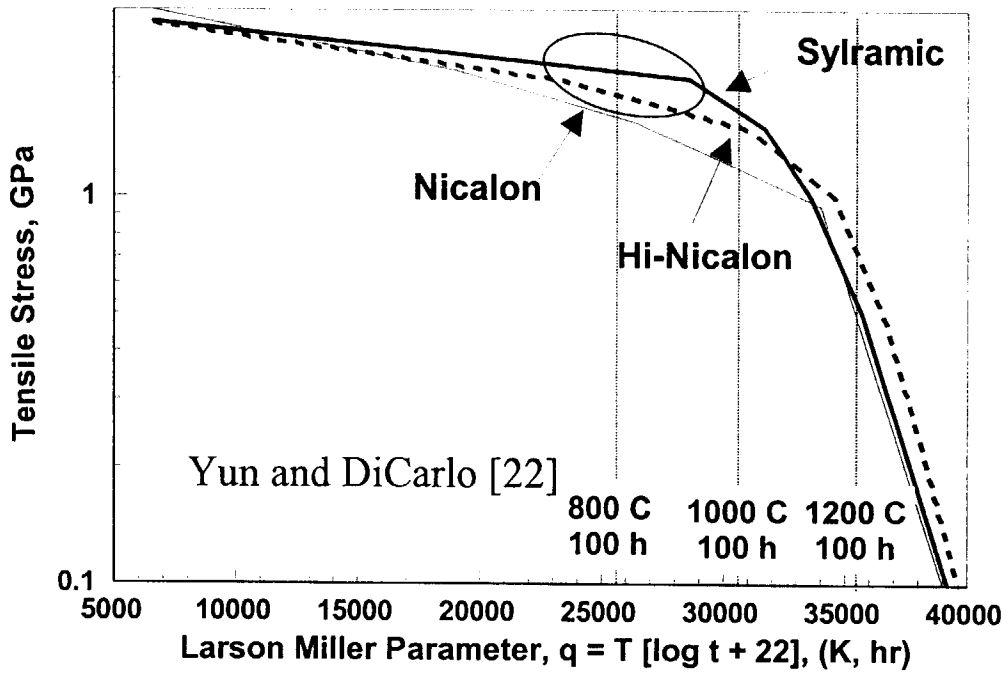

Figure 6: Rupture strength in a Larson-Miller format for different SiC fibers from Yun and DiCarlo [22].

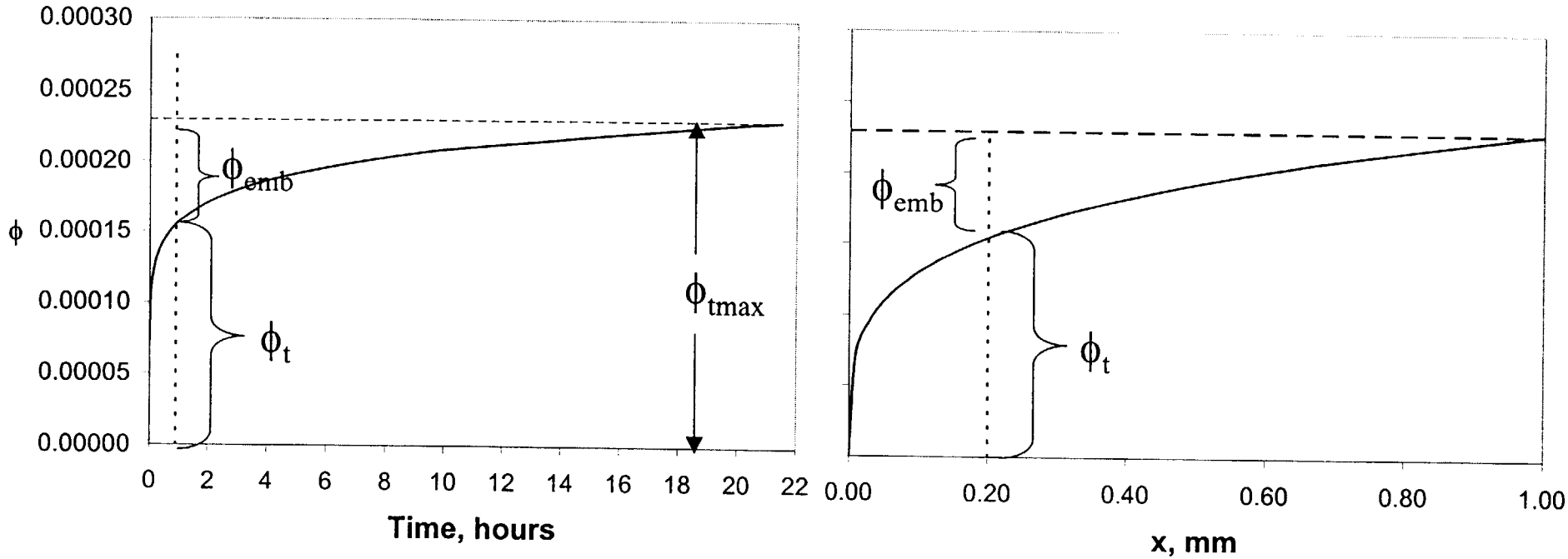

Figure 7: Predicted fraction of fiber failures for HN in a matrix crack of an HN-BN-MI composite at 815°C (Table I) as a function of (a) time and (b) embrittlement depth for an applied composite stress of 150 MPa.

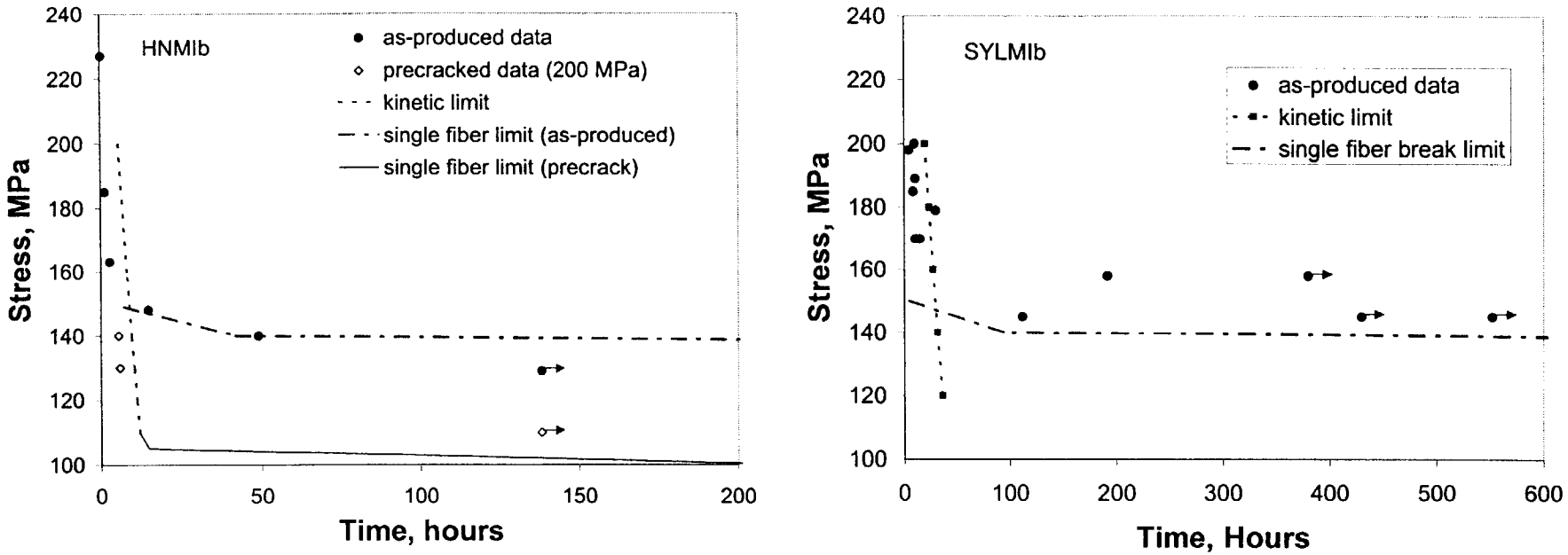

Figure 8: Stress-rupture at 815°C in air of BN interphase composites with (a) HN fibers and (b) SYL fibers.

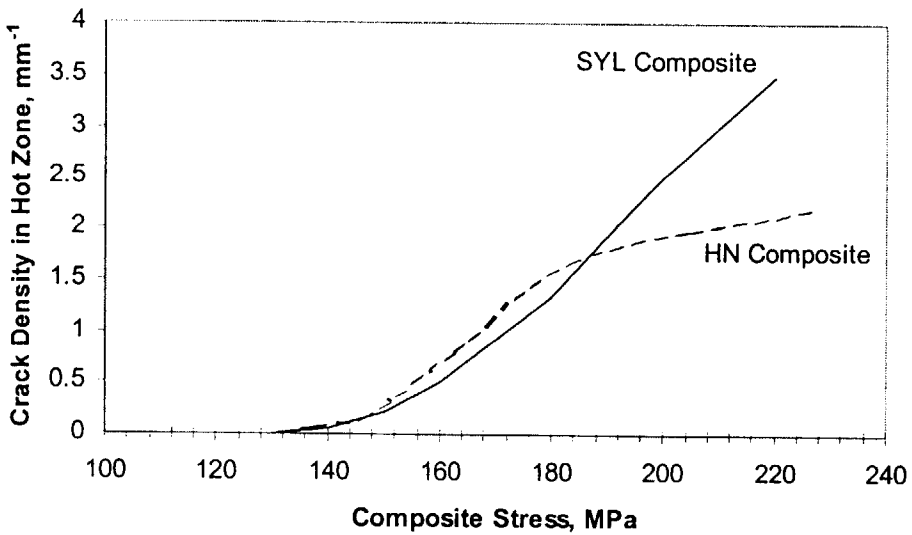

Figure 9: Stress-dependence for matrix crack density for SYL and HN composites. The curves were based on post-test measurements of failed specimens.

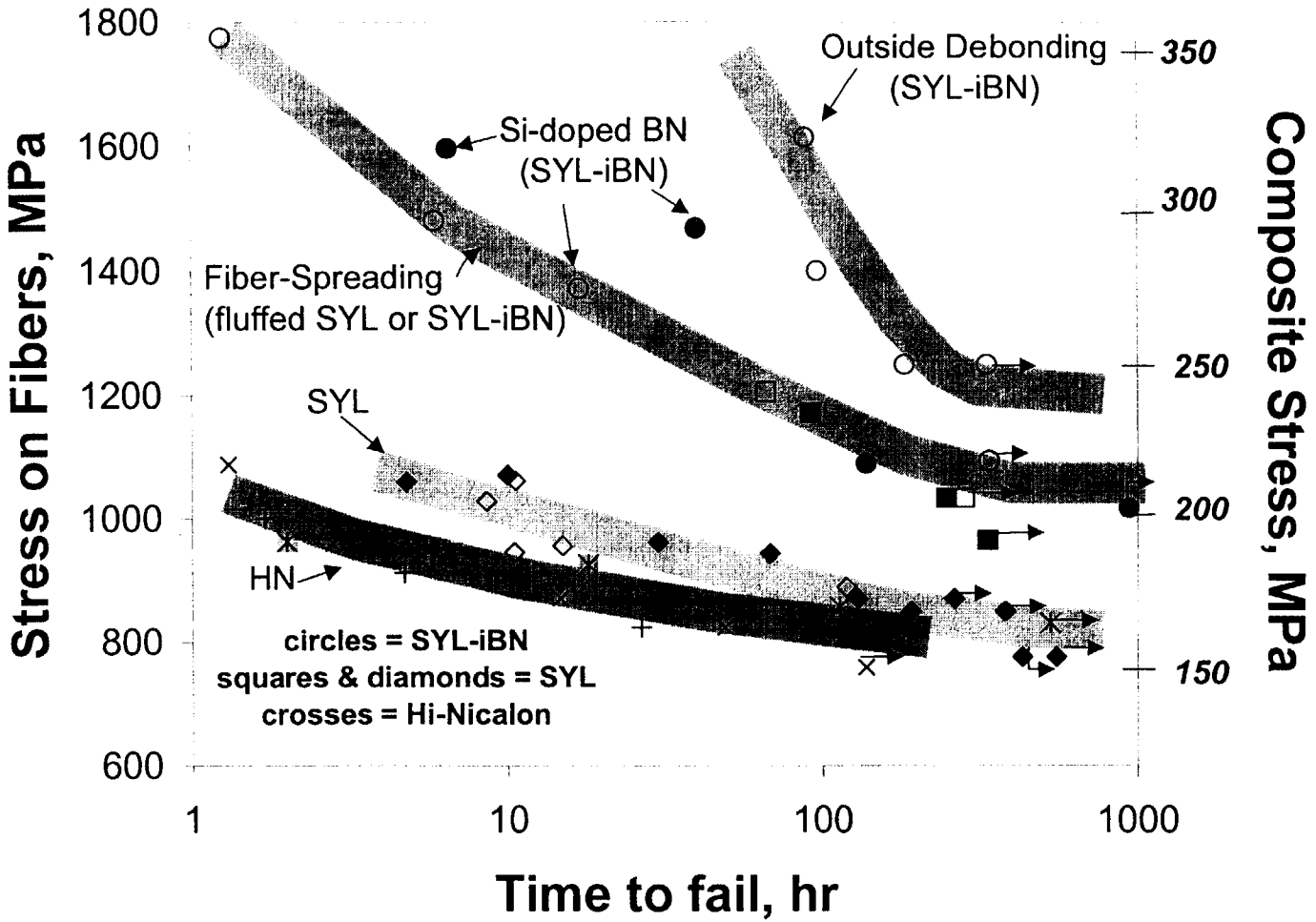

Figure 10: Stress-rupture properties at 815°C in air of conventional woven BN interphase composites and composites with interphase improvements.

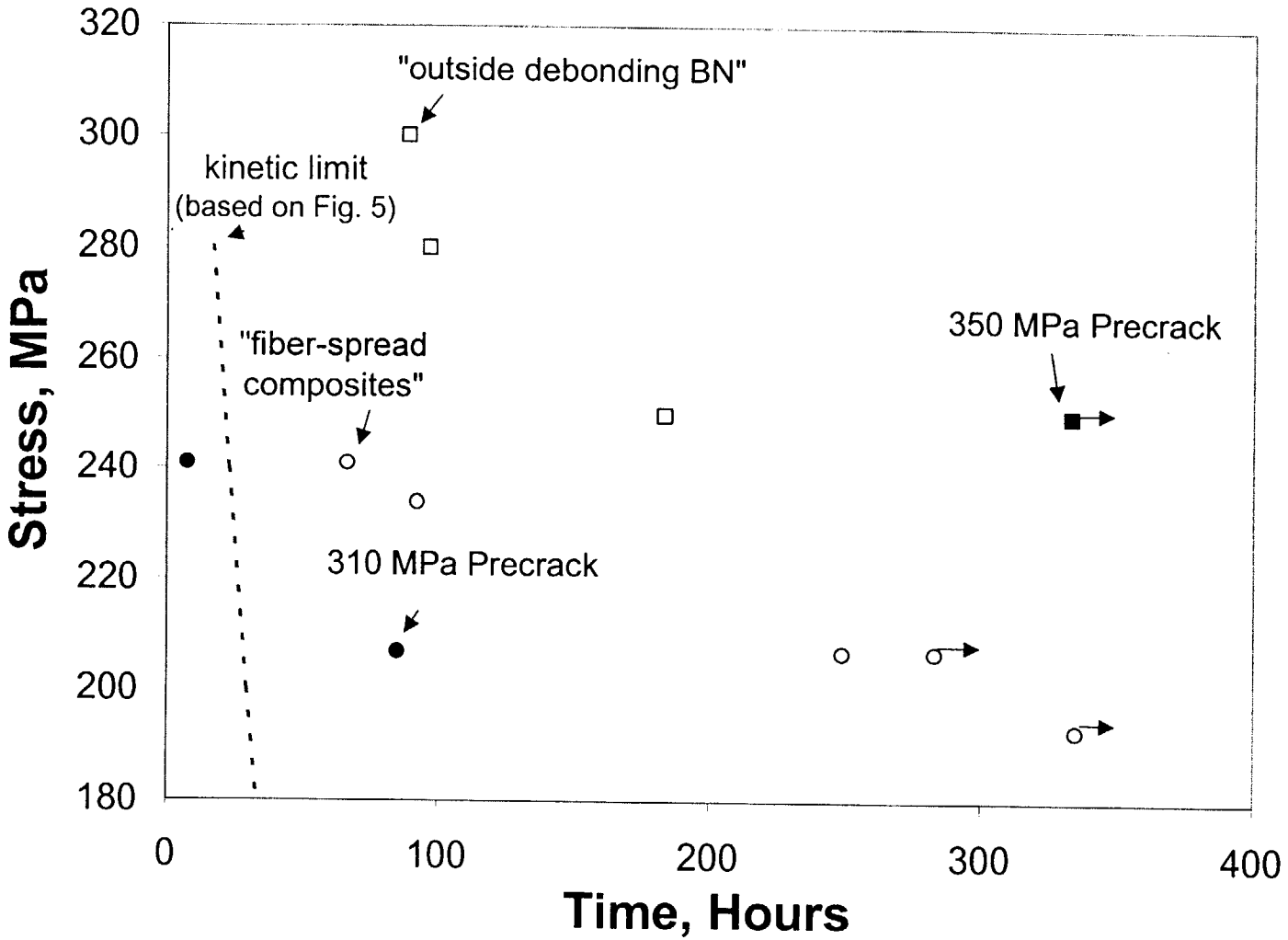

Figure 11: Stress-rupture of fiber-spread composite and outside-debonding BN composite. Both composites had a fiber volume fraction in the loading direction of 0.2.